Numerical Analysis of Charged Particles Transport in Air Based on Vortex Rings

MING ZHANG[1], **FENG HAN**[1], **PENGYU WANG**[1], **CHENGJIN QIAN**[1],
CHUAN LI[1], **(Member, IEEE), YONG YANG**[2], **(Member, IEEE),**
AND KEXUN YU[1]

[1]International Joint Research Laboratory of Magnetic Confinement Fusion and Plasma Physics, State Key Laboratory of Advanced Electromagnetic Engineering and Technology, School of Electrical Engineering and Electronics, Huazhong University of Science and Technology, Wuhan 430074, China
[2]State Key Laboratory of Advanced Electromagnetic Engineering and Technology, School of Electrical Engineering and Electronics, Huazhong University of Science and Technology, Wuhan 430074, China

Corresponding author: Chuan Li (lichuan@hust.edu.cn)

ABSTRACT Charged particles are widely used in the fields of defogging, haze removal and artificial rainfall. A novel transport strategy of charged particles based on the vortex rings is presented in this paper, to expand the effective action region and enhance the effect of charged particles. Transport distance and transport velocity (TV) of charged particles are the crucial two evaluation indexes. For the vortex rings generated by a piston-cylinder device, the transport velocity is closely related to Reynolds number and formation time. Based on the k-ω turbulence model, this paper verifies the relationship between vortex ring circulation, transport velocity and Formation Number in air by finite element methods, and studies the influence on the formation of vortex rings of an insulating bell mouth placed at the outlet of cylinder. The simulation results show that the Formation Number of vortex rings in the air is $4.0 \sim 5.0$, and the growth rate of transport velocity of vortex ring slows down when the formation time is larger than Formation Number. The study also indicates that the bell mouth has little effect on the velocity of the vortex ring, when the bell mouth angle is greater than $45°$ and the length of generatrix is between 0.2 m and 1.0 m. Therefore, the research results can provide a reference for the design and optimization of a vortex ring generator for transporting charged particles to a certain target area.

INDEX TERMS Charged particles, formation number, transport velocity, vortex ring.

I. INTRODUCTION

The application of charged particles in rain enhancement and fog elimination has attracted the attention of many researchers [1]–[4]. Khain *et al.* [3] report the charged particles could be transported by natural winds and updrafts. However, due to the limited diffusion of charged particles, the effective action region in these applications, is only restricted in the area near the charge generating device. The ion concentration decreases rapidly with spatial distance. Thus, to expand the action region, a suitable and highly efficient method to transport and diffuse the charged particles to a further area is crucial and anticipated.

Considerable research efforts have been devoted to the vortex ring, which is an effective transport carrier for particles.

The associate editor coordinating the review of this manuscript and approving it for publication was Md. Moinul Hossain.

Many vortex rings models under diverse conditions have been proposed [5]–[7]. Further, Domon *et al.* [8] confirm that the mass can be transported by water vortex rings based on a series of experiments. Yagami and Uchiyama [9], Uchiyama and Yagami [10] have studied the transport of solid particles by air vortex rings, and reveal that vortex ring can entrain or capture and then transport solid particles at a certain Stokes number ($\sim$0.01). Faulkner and Dvorsky [11] put forward a series of generator apparatus to produce vortex rings for transporting suspended ionized particles in the air, which implies the availability of charged particles transport by using vortex rings.

The key indicators to evaluate the effect of charged particles transport based on vortex ring, are the transport velocity (TV) and the transport distance of the vortex ring. According to the formula deduced by Shusser and Gharib [12], the TV is closely related to the circulation of vortex ring.

And Gharib *et al.* [13] have demonstrated that the circulation of vortex ring generated by a piston-cylinder device would reach the maximum in the water when the formation time (the ratio of piston stroke and piston diameter) lies in the range of 3.6 ∼ 4.5. Obviously, the TV of vortex ring is influenced by the formation time. Therefore, we must first verify the 'Formation Number' (FN) in the air, which makes the circulation reaches the maximum value.

Moreover, in order to create an area with high concentration charged particle at the outlet of the piston-cylinder device and reduce the disturbance on the vortex ring formed by the outside air flow, an insulating bell mouth is placed at the outlet. And Didden [14] indicate that the vorticity of vortex ring is derived from the separation of the shear layer at the outlet. That means the existence of bell mouth placed at the outlet, may weaken the strength and transport velocity of the vortex ring. However, Didden *et al.* don't investigate the specific influence of the outlet shape on the vortex ring propagation. Thus, this paper studies the effect of the bell mouth with various generatrix lengths and angles on the transport velocity of vortex ring, and aims to provide a reference for the design and optimization of the charged particle transport device based on vortex ring.

II. FORCE ANALYSIS OF CHARGED PARTICLES TRANSPORTED BASED ON VORTEX RING

During the transport evolutionary process of charged particles based on vortex ring, the following three forces are mainly involved: drag force, gravity and electrostatic force. The drag force formula is given as [15]

$$F_D = m_p \left(\boldsymbol{u} - \boldsymbol{v} \right) \big/ \tau_p \qquad (1)$$

$$\tau_p = \frac{4\rho_p d_p^2}{3\mu C_D \text{Re}_r} \qquad (2)$$

$$C_D = \frac{24}{\text{Re}_r}(1 + \frac{3}{16}\text{Re}_r) \qquad (3)$$

$$\text{Re}_r = \rho d_p \left| \boldsymbol{u} - \boldsymbol{v} \right| \big/ \mu \qquad (4)$$

where,

F_D - drag force;
m_p – mass of particle;
$\boldsymbol{u}$ - velocity of the fluid;
$\boldsymbol{v}$ - velocity of the entrained particles;
τ_p - particle velocity response time;
ρ_p - density of the particle;
d_p – diameter of particle;
μ - viscosity coefficient;
C_D - drag coefficient;
Re_r - particle Reynolds number;
ρ - density of the fluid.

The charged particles that are transported are usually water droplets and other aerosol particles. Taking a water particle with a diameter of 10 μm as an example, when the particles are stationary and the fluid velocity is 1.0 m/s, the drag force approximates 1.92×10^{-9} N by formulas (1) to (4).

Meanwhile, the gravity of water particles (diameter 10 μm) can be calculated as 5.13×10^{-12} N, based on the formula (5).

$$G = 4\rho\pi r^3 g \big/ 3 \qquad (5)$$

The saturated charge of a droplet can be given by

$$q_s = 8\pi \sqrt{\varepsilon_0 \sigma_s r^3} \qquad (6)$$

where, q_s is saturated charge, r is the radius of the suspended particles, ε_0 is the vacuum permittivity, σ_s is the surface tension of the suspended particles [16]. Thus, the saturated charge of the 10-μm particle is 2.24×10^{-13} C at room temperature (293.15K). Considering particles as point charges, according to Coulomb law, the value of electrostatic force between two particles is $4.6 \times 10^{-16}/r^2$, and r is the distance between two particles. It can be seen that the electrostatic force is on the order of 10^{-8} when the typical distance between the charged particles is about 100 μm [17], which can be also derived from the concentration of 10^4 cm^{-3} of water particles [18]. What's more, the actual charged ratio (the ratio of carried charge and Rayleigh limit) is no more than 10% [18], which will further reduce the order of electrostatic force.

Therefore, during the transport of charged particles, the drag force is much greater than both the electrostatic force and gravity. And it is reasonable to accept that the motion traces of charged particles are highly consistent with the streamlines of vortex ring motion [19]. The influence of forces other than drag force are no longer taken into consideration in the following simulation.
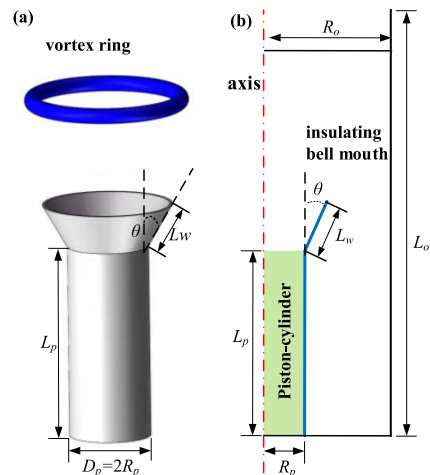

FIGURE 1. Schematic diagram of device and model. (a) Three-dimensional view of piston-cylinder device and (b) 2D axisymmetric model (not to scale).

III. SIMULATION OF AIR VORTEX RING

Gharib *et al.* [13] study the vortex ring generated by a piston-cylinder device in water and gave a definition of 'Formation Number'. In order to verify whether this conclusion also applies to the air vortex ring, this paper studies the vortex ring generated by the piston-cylinder device as shown in Fig. 1(a).

Based on 2D axisymmetric model of piston-cylinder device as shown in Fig 1(b), the generation and transport process are studied by using a RANS, k-ω model, focusing on the circulation and transport velocity (TV). The k-ω model solves the Navier-Stokes equations for conservation of momentum and the continuity equation for conservation of mass. The reference pressure and temperature are set to 1 atm and 293.15 K. Considering the small changes in pressure and temperature during the flow, incompressible flow is selected. Furthermore, the influence of various generatrix length and angle of bell mouth on the TV of vortex ring is also analyzed.

In Fig.1, D_p is piston diameter, R_p is piston radius, and L_p is the length of piston cylinder. The green shadow area is the piston-cylinder device. L_o and R_o are the length and radius of air calculation domain, respectively. The red dash-dotted line is the symmetry axis. Solid blue line indicates the insulating bell mouth. L_w and θ are generatrix the length and angle of insulating bell mouth, respectively. The motion of the piston is simulated by setting the inlet velocity function. When the inlet velocity function is a step function, the piston stroke (L_p) is equal to the piston velocity (V_p) multiplied by the piston movement time (t), i.e. $L_p = V_p t$.
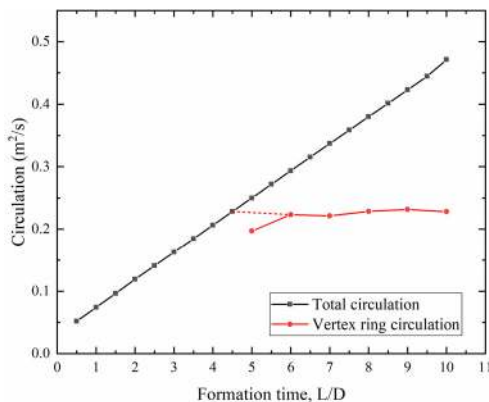

FIGURE 2. Total circulation and vortex ring circulation as a function of formation time (L/D) at D_p = 0.2 m.

IV. ANALYSIS OF SIMULATION RESULTS

A. FORMATION NUMBER

When the piston diameter (D_p) is 0.2 m, the piston velocity is 0.5 m/s and Reynolds number is 6,730 at the piston-cylinder device, the corresponding total circulation and vortex ring circulation are shown in Fig. 2. The maximum of vortex ring circulation is equal to the total circulation at L/D ≈ 4.5 (FN, as defined above), which is close to the experiment results of Gharib *et al.* [13]. Where, L is the equivalent stroke, and D is the diameter of the vortex ring generator outlet. Because the vortex ring generator in this paper is cylindrical, L is equal to the piston stroke $L_p = 4V/(\pi D^2)$, where, V is the volume of the vortex ring generator, and D= D_p. The breakdown point is identified when the vortex ring circulation do not increase with the value of L/D, which indicates that FN in the air is about 4.5.

When charged particles are transported by vortex ring, the transportation effect is mainly reflected by transport distance and transport velocity. The transport distance is defined as spatial distance between the center of the vortex core (maximum vorticity point) and the cylinder outlet. To better reflect the transport velocity of vortex ring, the slope of the linear fitting curve of the transport distance over time first 30 seconds after the piston stop moving, is defined as the average transport velocity (ATV) in this paper.
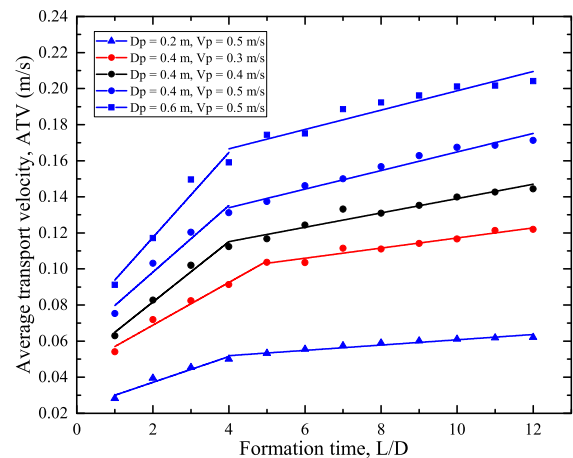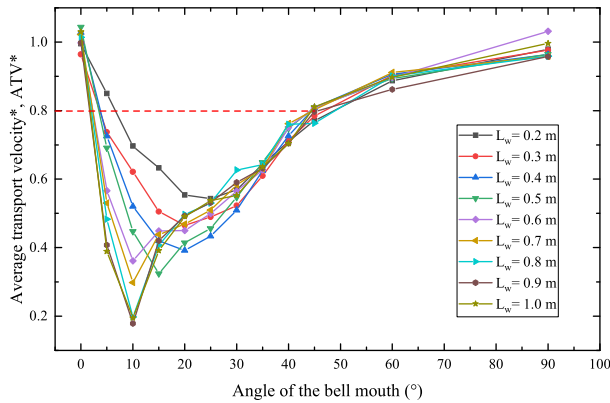

FIGURE 3. ATV of vortex ring as a function of formation time with various D_p (0.2 m, 0.4 m, 0.6m) and V_p (0.3 m/s, 0.4 m/s, 0.5 m/s).

The relationship between the simulated ATV of vortex ring and formation time is shown as in Fig. 3, and the straight lines are obtained by piecewise linear fitting. ATV increases with the formation time, but the growth rate of ATV slows down after the formation time exceed a value between 4.0 and 5.0, which appears in various combinations of piston diameter (D_p) and piston velocity (V_p). In addition, it should be noted that ATV increases with D_p under the identical V_p = 0.5 m/s, which can be concluded from the three blue lines in Fig. 3. Similarly, ATV has a positive relationship with V_p under the identical D_p = 0.4 m. As for the increase of ATV when the formation time is large than FN, it may be caused by the supplement from the vorticity of trailing jet. However, the destruction of the vortex ring may occur, if the vortex ring is caught up by trailing jet [13]. Therefore, to study on the vortex ring transport capacity, a stable and highly efficient vortex ring is necessary and it is a suitable choice to choose the formation time of vortex ring as 4.0 ∼ 5.0.

B. EFFECT OF GENERATRIX LENGTH AND ANGLE OF INSULATING BELL MOUTH

The insulating bell mouth's effect on the TV of the vortex ring is shown in Fig. 4 and Fig. 5. In the simulation, the Reynolds number of the vortex ring is 8,000, based on the diameter (0.4 m) and velocity (0.297 m/s) of piston, and moving time of the piston is 6.73 seconds. The corresponding formation time (L/D) is about 5.0 and illustrated as an inflection point as shown in Fig. 3. The normalized average transport velocity

FIGURE 4. ATV of vortex ring at different generatrix length (L$_W$) as a function of the angle of insulating bell mouth (θ) for the case of D_p = 0.4 m, Re = 8,000.
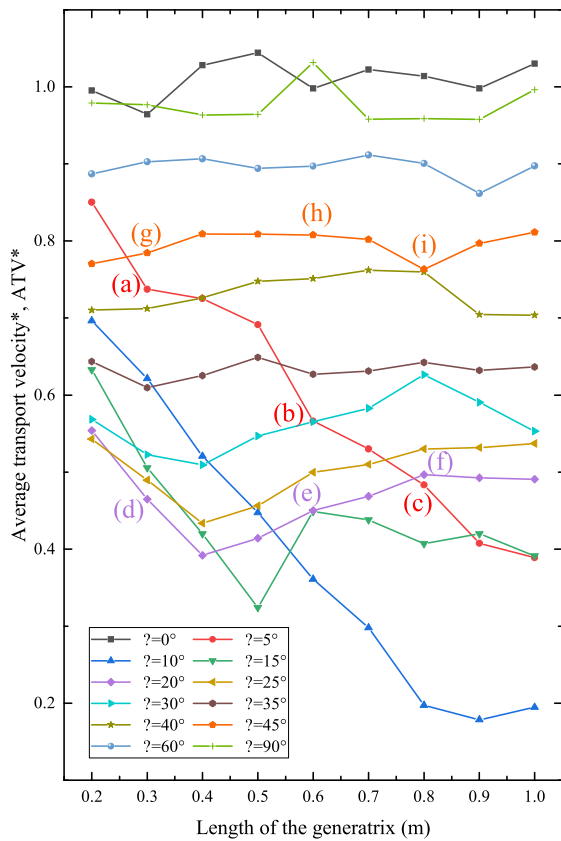
FIGURE 5. ATV of vortex ring at different angle (θ) as a function of the generatrix length (L$_W$) for the case of D_p = 0.4 m, Re=8,000.

ATV* = ATV/ATV', where ATV' represents the average value of ATV with angle 0° at various generatrix lengths (0.2 m ~ 1.0 m). Thus, ATV* of some points are larger than 1.0. The vorticity field of vortex ring corresponding to the points (a) ~ (i) in Fig. 5 are shown in Fig. 6(a) ~ (i), and the t is the time after the piston stopping.

As depicted in Fig. 4 and Fig. 5, ATV* of the vortex ring can be affected by the angle and generatrix length of bell mouth. ATV* decreases first and then increases with the angle
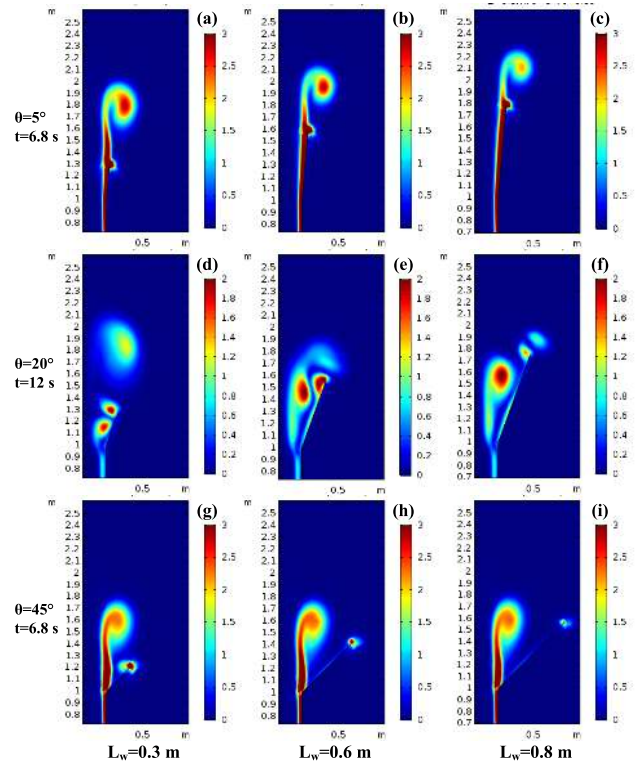
FIGURE 6. Vorticity field at different generatrix length and angle of insulating bell mouth (D$_p$ = 0.4 m, Re = 8,000).

of bell mouth. When the angle varies from 5° to 45°, the ATV* is less than 0.8. When the angles are 5° and 10°, the ATV* decreases with the generatrix length (L$_w$) as shown in Fig. 5, owing to the fact that the vortex ring forms at the outlet edge of the bell mouth as shown in Fig. 6(a) ~ (c).

However, when the angle is greater than 30°, the ATV* increases with the angle, and is unrelated to the generatrix length as shown in Fig. 5. That's because the forming point of vortex ring is transferred to the beginning of the bell mouth, that is, the cylinder outlet. For example, the vorticity fields with θ = 45°, L$_w$ = 0.3 m, 0.6 m and 0.8 m are shown in Fig. 6(g) ~ (i). It can be seen that vortex rings form at the beginning of the bell mouth, so the bell mouth has almost no adverse impact in the formation of vortex ring and the change of generatrix length no longer has a significant effect on the ATV*.

When the angle is between 15° and 30°, the ATV* decreases first and then increases with the generatrix length as shown in Fig. 5. That's because the vortex ring can be formed either at the beginning of the bell mouth or at the end of the mouth, even forming vortex rings at both the beginning and the end. This depends on the generatrix length of the bell mouth. With taking the interaction of different vortex rings formed at different position into consideration, the moments of Fig. 6(d), Fig. 6(e) and Fig. 6(f) are selected as 12 s, which is larger than that of the other figures (6.8 s), to obtain a stable state for descriptions. Taking θ = 20° as an example, when the generatrix length is 0.2 m ~ 0.4 m, the vortex ring forms at

the end of the bell mouth as shown in Fig. 6(d), and the ATV* decreases with the generatrix length. As for the generatrix length which is larger than 0.8 m, the vortex ring forms at the beginning of the bell mouth as shown in Fig. 6(f), and the ATV* is almost unaffected by the change of bell mouth length. In addition, it should be noted that when the generatrix length varies from 0.4 m to 0.8 m, the vortex rings will form at both the beginning and the end of the bell mouth as shown in Fig. 6(e). These two rings will affect each other, and the strength of vortex ring formed at the beginning of the bell mouth will increase with the generatrix length. That is the reason why ATV* increases as the generatrix length, when the generatrix length is between 0.4 m and 0.8 m.

V. CONCLUSION

A novel transport strategy of charged particles based on the vortex rings is presented in this paper. The numerical analysis has verified that Formation Number of vortex rings in the air is about $4.0 \sim 5.0$. The growth rate of average transport velocity (ATV) of vortex rings, which are formed at various Reynolds numbers and piston diameters, slows down after the formation time exceeds Formations Number. Therefore, to transport the charged particles by a stable and highly efficient vortex ring, the formation time of the vortex ring can be taken in the vicinity of Formation Number.

To reduce the disturbance on the vortex ring formed by the outside air flow and obtain a wide area with high concertation of charged particles, it is an approach to place an insulating bell around the charge generating device (eg. corona discharge). The effect on the vortex rings of the angle and generatrix length of insulating bell mouth has been investigated in detail. When the angles are $5°$ and $10°$, the ATV* decreases with the generatrix length (L_w). However, when the angle is greater than $30°$, the change of generatrix length will no longer have a significant effect on the ATV∗, owing to the transfer of the forming point of vortex ring. It's worth noting that the vortex ring can be formed either at the beginning of the bell mouth or at the end of the mouth, when the angle is between $15°$ and $30°$. According to the research results, the angle of the insulating bell mouth should be $45°$ or more to obtain a high-efficiency vortex ring. In this case, the ATV of vortex ring remains more than 80% of that without bell mouth, and the generatrix length will not cause the decay of the ATV.

REFERENCES

[1] Y. Yang, X. Tan, D. Liu, X. Lu, C. Zhao, J. Lu, and Y. Pan, "Corona discharge-induced rain and snow formation in air," *IEEE Trans. Plasma Sci.*, vol. 46, no. 5, pp. 1786–1792, May 2018.

[2] R. Chambers, S. Beare, S. Peak, and M. Al-Kalbani, "Using ground-based ionisation to enhance rainfall in the Hajar mountains, Oman," *Arabian J. Geosci.*, vol. 9, no. 7, pp. 1–16, Jun. 2016.

[3] A. Khain, V. Arkhipov, M. Pinsky, Y. Feldman, and Y. Ryabov, "Rain enhancement and fog elimination by seeding with charged Droplets. Part I: Theory and numerical simulations," *J. Appl. Meteorol.*, vol. 43, no. 10, pp. 1513–1529, Oct. 2004.

[4] H. Uchiyama and M. Jyumonji, "Field experiments of an electrostatic fog-liquefier," *J. Electrostatics*, vol. 35, no. 1, pp. 133–143, Jul. 1995.

[5] L. E. Fraenkel, "Examples of steady vortex rings of small cross-section in an ideal fluid," *J. Fluid Mech.*, vol. 51, no. 1, pp. 119–135, Jan. 1972.

[6] P. G. Saffman, "Dynamics of vorticity," *J. Fluid Mech.*, vol. 106, no. 3, pp. 49–58, 1981.

[7] I. S. Sullivan, J. J. Niemela, R. E. Hershberger, D. Bolster, and R. J. Donnelly, "Dynamics of thin vortex rings," *J. Fluid Mech.*, vol. 609, pp. 319–347, Aug. 2008.

[8] K. Domon, O. Ishihara, and S. Watanabe, "Mass transport by a vortex ring," *J. Phys. Soc. Jpn.*, vol. 69, no. 1, pp. 120–123, Jan. 2000.

[9] H. Yagami and T. Uchiyama, "Numerical simulation for the transport of solid particles with a vortex ring," *Adv. Powder Technol.*, vol. 22, no. 1, pp. 115–123, Jan. 2011.

[10] T. Uchiyama and H. Yagami, "Numerical simulation for the collision between a vortex ring and solid particles," *Powder Technol.*, vol. 188, no. 1, pp. 73–80, Dec. 2008.

[11] L. Faulkner and J. Dvorsky, "Generator apparatus for producing vortex rings entrained with charged particles," U.S. Patent 13 762 954, Aug. 22, 2013.

[12] M. Shsuser and M. Gharib, "Energy and velocity of a forming vortex ring," *Phys. Fluids*, vol. 12, no. 3, pp. 618–621, Mar. 2000.

[13] M. Gharib, E. Rambod, and K. Shariff, "A universal time scale for vortex ring formation," *J. Fluid Mech.*, vol. 360, pp. 121–140, Apr. 1998.

[14] N. Didden, "On the formation of vortex rings: Rolling-up and production of circulation," *Zeitschrift für Angew. Math. und Physik ZAMP*, vol. 30, no. 1, pp. 101–116, Jan. 1979.

[15] *Particle Tracing Module User's Guide: Particle Motion in a Fluid*, COMSOL Multiphys., Stockholm, Sweden, 2018.

[16] P. S. Maruvada, "Electric field and ion current environment of HVdc transmission lines: Comparison of calculations and measurements," *IEEE Trans. Power Del.*, vol. 27, no. 1, pp. 401–410, Jan. 2012.

[17] A. A. Fedorets, L. A. Dombrovsky, E. Bormashenko, and M. Nosonovsky, "On relative contribution of electrostatic and aerodynamic effects to dynamics of a levitating droplet cluster," *Int. J. Heat Mass Transf.*, vol. 133, pp. 712–717, Apr. 2019.

[18] P. Wang, C. Li, M. Zhang, Y. Yang, and K. Yu, "Density enhancement of nano-sized and submicron-sized water droplets induced by charges released from corona discharge," *J. Phys. D, Appl. Phys.*, vol. 53, no. 44, Oct. 2020, Art. no. 445203.

[19] M. Damak and K. K. Varanasi, "Electrostatically driven fog collection using space charge injection," *Sci. Adv.*, vol. 4, no. 6, Jun. 2018, Art. no. eaao5323.

MING ZHANG was born in 1980. He received the B.E., M.E., and Ph.D. degrees in electrical engineering from the Huazhong University of Science and Technology, Wuhan, China, in 2002, 2005, and 2008, respectively. He is currently a Professor with the School of Electric and Electronic Engineering, Huazhong University of Science and Technology. His current research interests include magnetic-confinement-fusion science and technologies and applications of low temperature plasma.

FENG HAN was born in Xinjiang, China, in 1995. He received the B.S. degree in energy and power from the Huazhong University of Science and Technology (HUST), Wuhan, China, in 2018, where he is currently pursuing the M.S. degree in electrical engineering. His current research interests include nucleation of charged particles and stability of charged droplets.

PENGYU WANG received the B.S. degree in electrical engineer and automation from the Wuhan University of Science and Technology, Wuhan, China, in 2015. He is currently pursuing the Ph.D. degree in electrical engineering with the Huazhong University of Science and Technology, Wuhan. His current research interests include mechanism of gas discharge and applications of low temperature plasma.

CHENGJIN QIAN was born in Hunan, China, in 1995. He received the B.S. degree in electrical engineering and automatization from the Huazhong University of Science and Technology (HUST), China, in 2017, where he is currently pursuing the M.S. degree in electrical engineering. His current research interests include high-power electronic switches and applications of low temperature plasma.

CHUAN LI (Member, IEEE) was born in Hubei, China, in 1989. He received the B.E. and Ph.D. degrees in electrical engineering from the Huazhong University of Science and Technology, Wuhan, China, in 2011, and 2016, respectively. He is currently working with the School of Electric and Electronic Engineering, Huazhong University of Science and Technology. His current research interests include fusion power supply engineering and applications of low temperature plasma.

YONG YANG (Member, IEEE) received the B.S. degree in engineering mechanics and the M.S. degree in electronics engineering from Tsinghua University, Beijing, China, in 2003 and 2006, respectively, and the Ph.D. degree in mechanical engineering from Drexel University, Philadelphia, PA, USA, in 2011. He is currently a Professor with the School of Electrical and Electronics Engineering, Huazhong University of Science and Technology, Wuhan, China, where he is working closely with the faculties and students with the Low Temperature Plasma Laboratory on atmospheric pressure plasmas in various media and their diagnostics.

KEXUN YU received the B.E., M.E., and Ph.D. degrees in electrical engineering from the Huazhong University of Science and Technology, Wuhan, China, in 1982, 1985, and 1989, respectively. He is currently with the State Key Laboratory of Advanced Electromagnetic Engineering and Technology, Huazhong University of Science and Technology. His research interests include high-performance electric drive systems and optimization design of electromagnetic devices.

● ● ●